

Received January 13, 2019, accepted February 16, 2019, date of publication February 27, 2019, date of current version March 13, 2019.

Digital Object Identifier 10.1109/ACCESS.2019.2901940

Robust Kalman Filter Algorithm Based on Generalized Correntropy for Ultra-Wideband Ranging in Industrial Environment

FUQIANG MA^{1,2}, JIE HE^{1,3}, (Member, IEEE),
AND XIAOTONG ZHANG^{1,2}, (Senior Member, IEEE)

¹Department of Computer Science and Technology, University of Science and Technology Beijing, Beijing 100083, China

²Beijing Advanced Innovation Center for Materials Genome Engineering, University of Science and Technology Beijing, Beijing 100083, China

³Beijing Key Laboratory of Knowledge Engineering for Materials Science, Beijing 100083, China

Corresponding authors: Jie He (hejie@ustb.edu.cn) and Xiaotong Zhang (zxt@ies.ustb.edu.cn)

This work was supported in part by the National Key Research and Development Program of China under Grant 2018YFB0704300, in part by the National Natural Science Foundation of China (NSFC) project under Grant 61671056, and in part by the Tianjin Special Program for Science and Technology under Grant 16ZXCXSF00150.

ABSTRACT The performance of time-of-arrival (TOA)-based ranging using ultra-wideband is greatly declined in the industrial environment since the metallic obstacles cause severe non-line-of-sight (NLOS) and result in huge ranging measurement errors. A general challenge of TOA-based ranging and localization in the industrial environment is that the Kalman filter (KF)-based ranging optimization algorithm cannot effectively improve the ranging accuracy because the ranging errors follow a non-Gaussian distribution. In this paper, a generalized maximum correntropy Kalman filter (GMCKF) algorithm which can effectively suppress NLOS errors is proposed. GMCKF uses the generalized maximum correntropy criterion (GMCC) instead of the minimum mean square error as the criterion of KF, and obtain a robust gain function. GMCC can effectively measure the similarity between the state value and the measurement value, which directly reflects the abnormality of measurement errors. Therefore, GMCKF achieves smoothing filtering in both NLOS and line-of-sight conditions. We compare GMCKF with other KF-based algorithms and prove its steady-state performance in field testing. The results show that the ranging optimized by GMCKF is with significantly higher accuracy. Finally, the optimized ranging is used as the input of three general localization algorithms. The localization accuracy of all localization algorithms is also improved.

INDEX TERMS Kalman filter, generalized maximum correntropy, LOS/NLOS, time-of-arrival.

I. INTRODUCTION

The indoor localization technology is one of the key technologies of internet of things (IoT), and it has been widespread concern by the researchers [1]. For example, many civil and military scenarios require accurate positioning information [3], [4], [43], such as search-and-rescue, looking for lost luggage, personal tracking, logistics tracking, and robot navigation, etc.

Localization based UWB ranging is one of the most frequently adopted technologies in the area of indoor positioning [5]. The main challenge of UWB ranging is the NLOS, in which the first arriving path is not related to the direct path and leads to large ranging measurement errors [39].

The associate editor coordinating the review of this manuscript and approving it for publication was Qinghua Guo.

Many research efforts have been spent on modeling and improving the performance of UWB ranging in office environment, in which the errors of UWB ranging are mainly caused by the obstacles, such as human bodies, office equipment, and walls [6]–[8]. With the development of industrial internet of things (IIoT), the industrial ranging technology is rising more and more attentions [2]. However, the error model of UWB ranging of industrial environment is considerably different from the office environment [38]. The walls of the factory are made of metal and the building is also packed with metallic equipment, such as machines and worktops. Because of large number of metallic objects, the probability of NLOS conditions is much higher in the industrial environment than in office environment.

In the practical environment, the measurement errors of UWB are mainly caused by multipath propagation, NLOS,

inaccuracy measurement of the equipment and so on [9]. The equipment measurement errors are caused by the time deviation between the clocks of the anchor node and tag node. Multipath propagation is composed of the reflection, refraction and diffraction of the wireless channel. Then, the arrival time of the direct path pulse may be shifted by the pulses of other paths, leads to multipath errors. In NLOS scenario, the direct path is usually blocked by the obstacles and becomes undetectable. For typical ranging systems, the NLOS errors are much larger than the multipath errors and equipment measurement errors [10]. The scenario of industrial UWB ranging is classified into LOS and NLOS. In LOS scenario, the ranging errors are composed by equipment measurement errors and multipath errors. In NLOS scenario, the ranging errors are composed by all three kinds of errors, much larger than the ranging errors of LOS. Usually, NLOS errors are unavoidable which lead to large positioning deviations, especially in industrial environment. Those NLOS errors exceed the standard deviations of Gaussian distribution. Therefore, the measurement results often contain large outliers, and the probability density functions (pdf) of NLOS errors decay with significant tailing which follow non-Gaussian distribution.

A general challenge of TOA based ranging and localization in industrial environment is that the Kalman filter (KF) based distance optimization algorithm cannot effectively improve the ranging accuracy when NLOS errors are modeled as Gaussian distribution. Meanwhile, second-order statistics of KF fail to describe error characteristics. Traditional methods of restraining NLOS include ranging scenario identification based adjusting [11], interacting multiple model (IMM) [12] and particle filtering (PF). The IMM algorithm must be modeled the LOS/NLOS switching in the Markov chain. If the LOS/NLOS modes of IMM do not match with discrete-time Markov chain, the performance will decrease seriously. The state estimation of PF is dependent upon the approximation between the reference distribution and the posterior probability distribution of state. In practice, it is difficult to obtain the optimal reference distribution.

On the other hand, kernel method [13] is widely studied because of its powerful nonparametric modeling ability. As a typical kernel method, maximum correntropy Kalman filter algorithm (MCCKF) can deal with the high order statistics of signal, thus eliminate the outliers, and achieve stable tracking and localization [14]. However, Gaussian kernel has not always been the best criterion. Recently, Chen *et al.* [15] proposes a generalized correntropy for robust adaptive filtering with the generalized Gaussian density (GGD) function, and achieves better performance than Gaussian kernel based robust adaptive filtering.

In order to improve the ranging accuracy of NLOS, a generalized maximum correntropy Kalman filter (GMCKF) algorithm is proposed. The generalized maximum correntropy criterion (GMCC) is a nonlinear similarity measure between two random variables in kernel space at any time and ignores the prior distribution of errors. GMCC takes place of MMSE

criterion as the cost function of the Kalman filter algorithm. Then, GMCC maximizes the similarity between the state value and measurement value, and can intuitively reflect the abnormality of NLOS errors. When the errors of NLOS follow non-Gaussian distribution, the Kalman filter will fail to compute the second order statistics of state value and measurement value. However, GMCC maps the input signal from a low dimensional space into a high dimensional space, and then processes the high order statistics of signal. Therefore, GMCC can not only suppress error of Gaussian distribution, but also be robust against errors of non-Gaussian distribution, such as alpha-stable distribution. When ranging results contain large outliers, GMCC makes the gain function of GMCKF small, and alleviate the contribution of the measurement value, that is, the predicted value approaches to the state value which means the smoothing filtering. The main contributions of this paper are as follows:

- 1) We propose a novel GMCKF algorithm, which is a robust nonlinear similarity measure and can effectively eliminate abnormal NLOS errors.
- 2) The effectiveness of this proposed algorithm is verified in different industrial scenarios, and it is concluded that GMCKF has superior performance in both LOS and NLOS conditions.
- 3) The practical localization performance for three representative algorithms are conducted by using the optimized ranging of GMCKF.

The rest of this paper is organized as follows. In Section II we briefly introduce related work. In Section III, we explain the error distribution. In Section IV we propose the generalized maximum correntropy Kalman filter algorithm. Section V shows experiments. Finally, Section VI concludes this paper.

II. RELATED WORK

There are many radio frequency based localization methodologies, including received signal strength indicator (RSSI) [16], time of arrival (TOA) [17], time difference of arrival (TDOA) [18], angle of arrival (AOA) [19]. The ranging based on TOA is to calculate the distance between the transmitter and receiver by measuring the propagation time. The ranging accuracy is limited by the transmission condition of the wireless channels. If there is a LOS condition between the anchor node and tag node, the ranging accuracy of TOA will be higher. Otherwise, the TOA measurement will introduce the NLOS errors. In the industrial application, the serious NLOS scenarios result in the substantial measurement errors. Therefore, in order to achieve higher ranging accuracy for NLOS, it is necessary to eliminate the NLOS errors [20]. The related work of NLOS is introduced in the following.

The literature [22] proposes a directional beacon based UWB location method which uses correlation window and directional beacon to solve the influence of multipath and NLOS. The dynamic Gaussian model (DGM) [42] considers the instantaneous LOS or NLOS errors at time domain as the drift from the general distribution dynamically in the

indoor scenario. The Navigation Satellite System (GNSS) detection algorithm [41] uses the cooperative positioning (CP) techniques to improve the positioning accuracy of vehicles in urban NLOS environment. CP usually adopts the relatively accurate local measurements between vehicles, such as UWB, to enhance GNSS robustness.

Because the error distribution of NLOS and LOS channels is different, the NLOS and LOS channels are identified separately and use corresponding methods to reduce the propagation errors [23]–[25]. These methods usually adopt common strategies, such as estimating the variance of the distance, the statistical characteristics of the channel. Guvenc *et al.* [21] proposes a NLOS identification method with the amplitude and delay statistics of the UWB channel. The amplitude statistics are characterized by the kurtosis, and the delay statistics usually contain the mean excess delay and the root mean square delay spread. Channel classification Kalman Filter (CC-KF) [10] divides errors into three different classes based on the characteristics of ranging errors. It needs prior knowledge of error distribution. For example, ranging errors of CC-KF should be modeled as detected direct-path-pulse (D-DPP) error distribution or undetected-direct path pulse (U-DPP) error distribution.

Because it is difficult to distinguish NLOS with LOS channels, the measurement errors can be modeled and corrected directly. A correction algorithm based on information fusion algorithm is proposed [26]. The literature [27] proposes a blind selection method for direct path monitoring to solve the NLOS problem. The literature [28] sets up a special data model for UWB ranging to solve the NLOS problem. The error correction algorithm based on statistical theory and machine learning is proposed [29], [30], which needs to establish the appropriate statistical model to achieve good performance.

The interacting multiple model (IMM) estimator is a Markov based method when the ranging estimation contains LOS and NLOS errors. Li *et al.* [31] develops sequentially multi-sensor multi-model filter for a mixed LOS/NLOS environment which combines the IMM approach with the extended Kalman filter (EKF) technique. A concatenated IMM algorithm [12] takes the different dynamic models into the second Markov chain under LOS/NLOS environment, and this method is a hybrid Markov process which is composed of inner and outer layered IMM. M-estimation and IMM are combined to describe the mobile terminal tracking which can effectively trade off the LOS and NLOS environment [32]. When the errors are LOS distribution, the conventional EKF is adapted. Otherwise, the robust EKF (REKF) is used to mitigate the influence of NLOS errors.

The classical methods based on Monte Carlo (MC) use the probability distribution characteristics to suppress NLOS. Monte Carlo sampling can maintain the mean and variance characteristics of NLOS scenario, such as unscented Kalman filter (UKF), particle filter (PF) [33], [34]. UKF eliminates errors through the collection of sampling points, which will increase the computational complexity and cannot be well

applied to the real-time localization system. Yang [35] proposes the PF algorithm to realize the compromise between the ranging accuracy and the computational complexity. In addition, PF dynamically adjusts maps to improve the ranging accuracy.

Since errors of TOA ranging have a heavy tailed distribution under the NLOS condition, the Gaussian distribution cannot effectively explain the error model. Supposing observation noise follows a skew t-distribution, a light sigma-point Kalman filtering method can effectively treat LOS/NLOS condition of TOA [36]. The maximum correntropy Kalman (MCCKF) combines maximum correntropy criterion and the weighted least squares together to suppress NLOS errors. The MCCKF does not require any prior information and has lower computation [14]. Chen *et al.* [37] proposes a fixed-point Kalman filter algorithm based on the maximum correntropy which achieves a good ranging accuracy. However, the complexity is high due to its iterative procedure.

The aforementioned filtering algorithms for NLOS condition have improved the performance from different ways. However, there still exist some problems. 1). Some algorithms require additional hardware or assistant method to deal with NLOS errors which increase the complexity. 2). When the model does not match with the actual distribution, these algorithms based on the channel classification or the transition probability model will increase the ranging errors. 3). Some algorithms have a large computational complexity and cannot be well applied to the real-time localization system.

III. TOA RANGING PRINCIPLE AND ERROR MODEL

A. TOA RANGING PRINCIPLE

For TOA ranging, the greater the bandwidth is, the stronger the ability to suppress multipath interference. Therefore, this paper chooses UWB as a measuring chip, such as DW1000 [40]. Two way TOA (TW-TOA) does not require the time synchronization between the anchor node and tag node, and it can eliminate the time synchronization error in TOA ranging.

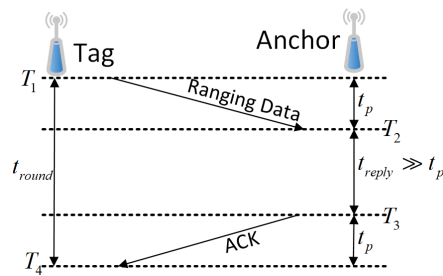


FIGURE 1. Diagram of the TOA principle.

As shown in Fig.1, *Anchor* and *Tag* are two nodes for TOA ranging. Tag node sends ranging data to anchor node at time T_1 . Anchor node receives information at time T_2 . Then, anchor node sends ACK data to tag node at time T_3 . Finally, tag node receives ACK data at time T_4 . Anchor and tag nodes measure the time of the transmission and reception

by the local clock, and the transmission time between the two devices is derived. The ranging between the anchor and tag node is as follows:

$$\hat{d} = t_p * c = \frac{t_{\text{round}} - t_{\text{reply}}}{2} * c = \frac{(T_4 - T_1) - (T_3 - T_2)}{2} * c \quad (1)$$

where c is the speed of light.

B. ERROR DISTRIBUTION ANALYSIS OF LOS AND NLOS

In the industrial environment, a large number of metallic devices cause severe NLOS transmission. In order to effectively analyze the impact of factory environment on UWB ranging, we set up the error model as follows:

$$e = d_{\text{true}} - \hat{d} = e_{\text{los}} + \delta_{\text{nlos}} e_{\text{nlos}} + e_d \quad (2)$$

where e represents the TW-TOA ranging error between the anchor node and tag node, d_{true} is actual ranging between the anchor node and tag node, e_{los} is measurement error caused by LOS condition, e_d is the error of hardware and other factors, e_{nlos} is NLOS error causing by buildings, equipment or other objects. When there is LOS condition between the anchor node and tag node, $\delta_{\text{nlos}} = 0$; otherwise, $\delta_{\text{nlos}} = 1$.

In order to effectively study the effect of measurement error, we use the industrial ranging data to calculate the distribution. The test is divided into two cases: one has equipment occlusion and the other can be regarded as LOS condition.

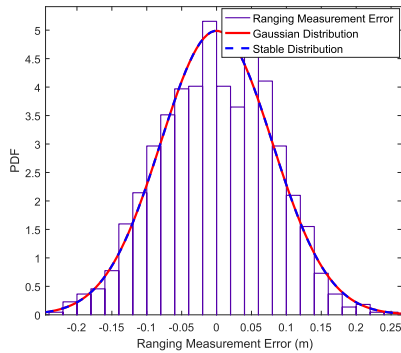


FIGURE 2. Error probability distribution under LOS scenario.

When there is LOS scenario between the anchor node and tag node, the error distribution is shown as Fig.2. The columnar graph represents the actual error data. The red curve indicates Gaussian distribution, and the blue curve indicates alpha-stable distribution. It can be seen that the most of errors are near zero, and the whole errors are closer to Gaussian distribution. At the same time, it is surprising to find that Gaussian distribution coincides with alpha-stable distribution, and the errors do not have heavy tailing. Note that Gaussian distribution is a special case of alpha-stable distribution. LOS error and hardware error can be effectively solved by traditional filtering algorithm which is considered as Gaussian distribution. It shows that the UWB is capable of resisting multipath interference and system deviation.

When there is NLOS scenario between the anchor node and tag node, the error distribution is shown as Fig.3.

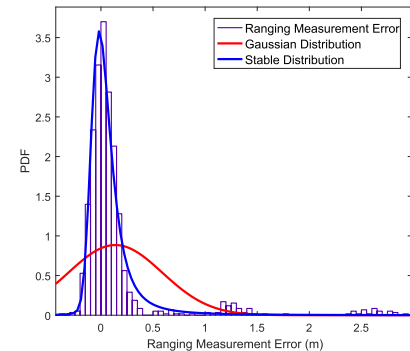


FIGURE 3. Error probability distribution under NLOS scenario.

Although the errors are mainly concentrated in zero, a few errors have heavy tailing which mean large outliers. Therefore, the whole distribution is similar to alpha-stable distribution which can provide a powerful model estimation for NLOS errors. The error distribution cannot be effectively characterized by Gaussian distribution. Note that Levy distribution is a special case of alpha-stable distribution which also has heavy tailing. The experiment results show that the ranging accuracy of UWB is mainly affected by NLOS condition. This paper is focus on suppressing NLOS errors and makes the ranging results closer to actual value.

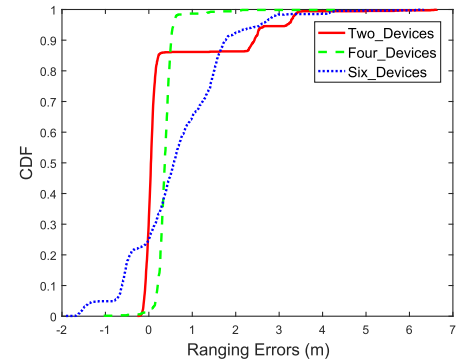


FIGURE 4. CDF of ranging errors with different metallic equipment.

When there are different metallic equipment between the anchor node and tag node, the cumulative distribution function (CDF) is shown as Fig.4. Because there are various multipath propagation conditions, the error distribution is not proportional to the number of obstacles. A general problem of the TOA approach is that the performance of ranging systems decreases rapidly in NLOS conditions since the first arriving path may not correspond to the direct path and includes an additional detouring delay.

IV. GENERALIZED MAXIMUM CORRENTROPY KALMAN FILTER (GMCKF)

A. GENERALIZED MAXIMUM CORRENTROPY CRITERION (GMCC)

The generalized correntropy is a new method for nonlinear and local similarity measure between two random variables

X and Y . It is defined as follows:

$$V(X, Y) = E_{XY}[\kappa(X, Y)] = \iint \kappa(x, y)p_{X,Y}(x, y)dxdy \quad (3)$$

$E[\cdot]$ is the expectation operator, $\kappa(\cdot, \cdot)$ is a translation function of shift-invariant Mercer kernel, $p_{X,Y}(\cdot, \cdot)$ is the joint probability density function of X and Y .

In this paper, the generalized Gaussian density (GGD) is used as kernel function:

$$\begin{aligned} \kappa(x, y) &= G_{\alpha, \beta}(x - y) = \frac{\alpha}{2\beta\Gamma(1/\alpha)} \exp(-|\frac{x-y}{\beta}|^\alpha) \\ &= \gamma_{\alpha, \beta} \exp(-\lambda|x-y|^\alpha) \end{aligned} \quad (4)$$

where $\alpha > 0$ is the shape parameter, $\beta > 0$ is kernel bandwidth, $\lambda = 1/\beta^\alpha$ is the kernel parameter, $\gamma_{\alpha, \beta} = \alpha/(2\beta\Gamma(1/\alpha))$ is the normalization constant, $\Gamma(\cdot)$ is the gamma function.

The generalized Gaussian density function has more free choices of parameters than Gaussian kernel function, and can be more effective to deal with non-Gaussian errors. When the parameters are suitable, it has a better performance. Therefore, this paper considers the generalized Gaussian density function as the kernel function.

B. GENERALIZED MAXIMUM CORRENTROPY KALMAN FILTER

Aiming at the problem that the accuracy of UWB ranging is significantly affected by NLOS errors in industrial environment, a novel method for NLOS errors based on KF is designed by using the generalized maximum correntropy as a cost function.

When the errors are non-Gaussian, the performance of KF will degrade significantly. In order to mitigate these drawbacks, we use GMCC to improve the robustness of KF. Due to the local similarity measure of GMCC, GMCKF can effectively eliminate NLOS errors.

The state model of a dynamic linear system is considered as follows:

$$x_k = Fx_{k-1} + w_k \quad (5)$$

$$y_k = Hx_k + v_k \quad (6)$$

where $F = [1, 1; 0, 1]$ is the 2×2 state matrix and $H = [1, 0]$ is the 1×2 measurement matrix. $x_k = [d_k, v_k]^T \in R^2$ and $y_k \in R$ represent the state value and measurement value respectively where d_k denotes the distance and v_k denotes the velocity of target node. w_k and v_k represent the state and measurement noise which has zero mean with covariance matrices Q_k and R_k , respectively.

GMCC is a nonlinear similarity measure between two random variables in kernel space at any time and ignores the prior distribution of errors. GMCC takes the place of the traditional MMSE criterion as the cost function of the Kalman filter algorithm. Then, GMCC maximizes the similarity between the state value and measurement value, and can intuitively reflect the abnormality of NLOS errors. In order to effectively suppress the NLOS errors, we combine GMCC and weight

matrix $R_k^{-1}, P_{k|k-1}^{-1}$ as the cost function.

$$J_m = G_{\alpha, \beta}(\|y_k - Hx_k\|_{R_k^{-1}}) + G_{\alpha, \beta}(\|x_k - Fx_{k-1}\|_{P_{k|k-1}^{-1}}) \quad (7)$$

Using generalized Gaussian density (GGD) as cost function, the solution may not be optimal and may be suboptimal. The domain of cost function (7) is $x_k \in \{H^{-1}y_k, Fx_{k-1}\}$ if $H^{-1}y_k < Fx_{k-1}$. State value x_{k-1} and measurement value y_k in the cost function can be regarded as fixed values at time t . In addition, the cost function J_m is bounded in its domain and there exists an updating predicted value x_k between $H^{-1}y_k$ and Fx_{k-1} that maximizes the cost function J_m and minimizes the error between real value and predicted value. The main purpose of this paper is to measure the similarity between the predicted value and the measurement value by using the generalized maximum correntropy criterion (GMCC). We can calculate the derivative of x_k :

$$\begin{aligned} &\frac{\partial J_m}{\partial x_k} \\ &= \frac{\partial (\exp(-\lambda|y_k - Hx_k|^{\alpha/2} R_k^{-1} |y_k - Hx_k|^{\alpha/2}))}{\partial x_k} \\ &+ \frac{\partial (\exp(-\lambda|x_k - Fx_{k-1}|^{\alpha/2} P_{k|k-1}^{-1} |x_k - Fx_{k-1}|^{\alpha/2}))}{\partial x_k} = 0 \end{aligned} \quad (8)$$

The expansion of (8) can be expressed:

$$\begin{aligned} &G_{\alpha, \beta}(y_k - Hx_k) H^T R_k^{-1} |y_k - Hx_k|^{\alpha-1} \text{sign}(y_k - Hx_k) - G_{\alpha, \beta} \\ &\times (x_k - Fx_{k-1}) P_{k|k-1}^{-1} |x_k - Fx_{k-1}|^{\alpha-1} \text{sign}(x_k - Fx_{k-1}) = 0 \end{aligned} \quad (9)$$

where $\text{sign}(\cdot)$ is sign function. $G_{\alpha, \beta}(\cdot)$ is GGD function which can reference to (4). We set $L_k = \frac{G_{\alpha, \beta}(y_k - Hx_k)}{G_{\alpha, \beta}(x_k - Fx_{k-1})}$. Then, $y_k - Hx_k$ and $x_k - Fx_{k-1}$ have the same symbols, equation (9) can be rewritten as:

$$L_k H^T R_k^{-1} (y_k - Hx_k)^{\alpha-1} = P_{k|k-1}^{-1} (x_k - Fx_{k-1})^{\alpha-1} \quad (10)$$

In order to effectively analyze the variable x_k , we take the $\alpha - 1$ root for both sides of (10) where $\alpha > 1$.

$$(L_k H^T R_k^{-1})^{1/(\alpha-1)} (y_k - Hx_k) = P_{k|k-1}^{-1/(\alpha-1)} (x_k - Fx_{k-1}) \quad (11)$$

We can transform (11) to (12). In order to obtain the optimal state estimation, we add and subtract an estimated value $(L_k H^T R_k^{-1})^{1/(\alpha-1)} Hx_{k|k-1}$ on the right side of (12):

$$\begin{aligned} &((L_k H^T R_k^{-1})^{1/(\alpha-1)} H + P_{k|k-1}^{-1/(\alpha-1)}) x_k \\ &= (L_k H^T R_k^{-1})^{1/(\alpha-1)} y_k + P_{k|k-1}^{-1/(\alpha-1)} x_{k|k-1} \\ &+ (L_k H^T R_k^{-1})^{1/(\alpha-1)} Hx_{k|k-1} - (L_k H^T R_k^{-1})^{1/(\alpha-1)} Hx_{k|k-1} \end{aligned} \quad (12)$$

We can transform (12) to (13):

$$\begin{aligned} &((L_k H^T R_k^{-1})^{1/(\alpha-1)} H + P_{k|k-1}^{-1/(\alpha-1)}) x_k \\ &= ((L_k H^T R_k^{-1})^{1/(\alpha-1)} H + P_{k|k-1}^{-1/(\alpha-1)}) x_{k|k-1} \\ &+ (L_k H^T R_k^{-1})^{1/(\alpha-1)} (y_k - Hx_{k|k-1}) \end{aligned} \quad (13)$$

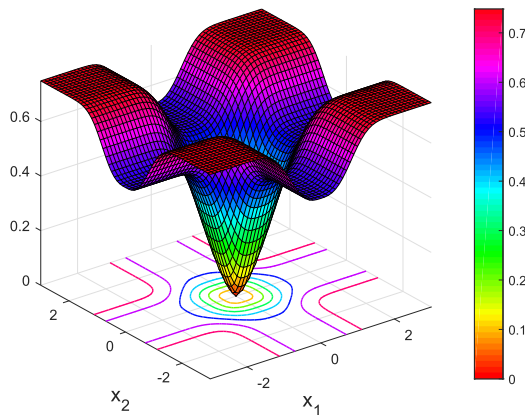


FIGURE 5. Surface of the GCIM in 3D space ($\alpha = 3, \beta = 1$).

Then, we set the gain K_k :

$$K_k = ((L_k H^T R_k^{-1})^{1/(\alpha-1)} H + P_{k|k-1}^{-1/(\alpha-1)})^{-1} (L_k H^T R_k^{-1})^{1/(\alpha-1)} \quad (14)$$

The essential difference between GMCKF and traditional KF is that the gain K_k of GMCKF contains L_k . When the measurement value contains NLOS errors, L_k can dynamically adjust the gain K_k of GMCKF and make the predicted value tend to state value. When the measurement errors follow Gaussian distribution, the gain K_k can be reduced to the traditional KF approximately.

Assume that R_k is $m \times m$ matrix, $P_{k|k-1}$ is $n \times n$ matrix, H is $m \times n$ matrix. Because operation of GMCKF is linear, L_k is scalar. K_k does not cause much computing complexity with the generalized Gaussian density (GGD). The gain K_k need $O(m^3 + n^3 + nm^2 + mn^2 + mn + m^2)$ operation.

The optimal state value can be expressed as follows:

$$x_k = x_{k|k-1} + K_k(y_k - Hx_{k|k-1}) \quad (15)$$

x_k can be approximately equal to $x_{k|k-1}$ in the denominator of L_k according to [14], so that $G_{\alpha,\beta}(x_k - Fx_{k|k-1}) \approx G_{\alpha,\beta}(x_{k|k-1} - Fx_{k|k-1}) = 1$. Finally, L_k can be expressed as:

$$L_k = G_{\alpha,\beta}(y_k - Hx_{k|k-1}) \quad (16)$$

The generalized correntropy induced metric (GCIM) is defined in [15] where $GCIM(X, Y) = \sqrt{G_{\alpha,\beta}(0) - V(X, Y)}$, $X = [x_1, \dots, x_N]^T$, $Y = [y_1, \dots, y_N]^T$. The surface of the GCIM is shown as Fig.5 where $X = [x_1, x_2]^T$, $Y = [0, 0]^T$, $\alpha = 3, \beta = 1$. The GCIM exhibits like different norm properties (from L_α to L_0) in different regions. These characteristics can refer to [15, Property 7 and 8]. It proves that GCIM is equivalent to the α -norm distance if two variables of $\{y_k, Hx_k\}$ or $\{x_k, Fx_{k|k-1}\}$ are close, behaves similarly to the 1-norm distance as two variables get further apart and eventually approaches the zero-norm as they are far apart. GMCC maps the input signal from a low dimensional space into a high dimensional space, and then processes the high order statistics of signal. Therefore, GMCC can not only suppress errors of Gaussian distribution, but also effectively be robust

against errors of non-Gaussian distribution, such as alpha-stable distribution. When measurement value contains large outliers, GMCC makes the gain function of GMCKF small, and alleviate the contribution of the measurement value, that is, the predicted value approaches to the state value which means the smoothing filtering.

GMCKF first predicts state value $x_{k|k-1}$ and covariance $P_{k|k-1}$, respectively. Then, the gain K_k is calculated by using GMCC function. Finally, GMCKF can obtain the filtering state value x_k and covariance P_k with K_k , $x_{k|k-1}$, and $P_{k|k-1}$. GMCKF algorithm is summarized as Fig.6:

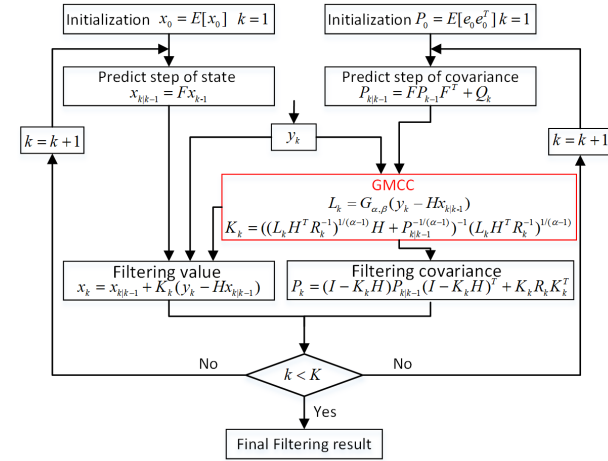


FIGURE 6. The diagram of GMCKF algorithm.

V. EXPERIMENTS

In order to effectively evaluate the performance of this proposed algorithm, TOA ranging uses the UWB system to verify its performance in the practical factory environment. First, the setting of experiment scenario is introduced, and the practical experiments are carried out on the different algorithms.

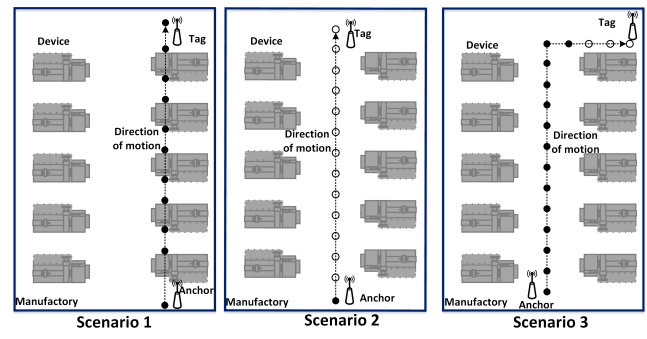


FIGURE 7. Experiment scenario for three cases.

A. MEASUREMENT SCENARIO

As shown in Fig.7, the practice measurement scenario is a factory containing many industrial machines. The test device consists of an anchor node, a tag node, and a laptop. The laptop receives ranging data and performs filtering algorithms. Fig.7 shows that both anchor node and tag node are deployed



FIGURE 8. Practice experiment scenario for NLOS and LOS.

on a tripod at one meter above the floor. The anchor node is fixed, the tag node moves with uniform speed and gets away from the anchor node. The experiment scenarios can be divided into three cases. Scenario 1 can be seen as a typical NLOS condition, and measurement errors follow alpha-stable distribution as shown in Fig.3. There is always an occlusion between the tag node and anchor node, and UWB signal is propagated by multipath way. Scenario 2 is LOS model, and measurement errors follow Gaussian distribution as shown in Fig.2. Scenario 3 can be regarded as a mixed model of LOS and NLOS. Three scenarios describe the various ranging conditions in the factory environment effectively and comprehensively. The following will focus on scenario 1 and scenario 2. Fig.8 shows the practical factory ranging scenario under LOS and NLOS conditions.

B. EXPERIMENT AND ANALYSIS

In each experiment, the tag node moves away from anchor node with 0.5m/s. 300 MC samples are carried out in each scenario. We consider the root mean square error (RMSE) and CDF as criterion to evaluate the performance of algorithms. We compare the GMCKF algorithm with the original KF, modified correntropy Kalman filter (MCKF) [14], and MCCKF [14].

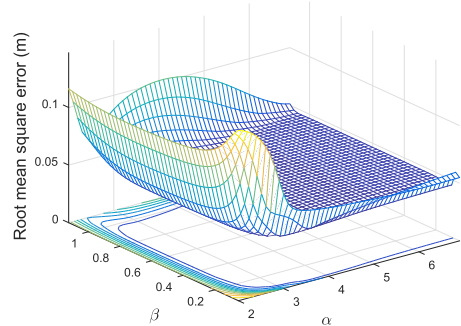


FIGURE 9. Joint distribution of α and β under NLOS condition.

1) STEADY-STATE PERFORMANCE UNDER NLOS CONDITION
The kernel parameters of GMCC is usually determined by cross-validation, nearest neighbors, Silverman's rule and so on [13], [15]. In order to prove the steady-state performance of GMCKF, we have tested the effects of parameters α and β on the performance in the scenario 1. Fig.9 indicates RMSE of GMCKF under the joint distribution of α and β .

From Fig. 9, when there is effect of NLOS, the optimal performance is achieved with $\alpha \in [3, 5]$ and $\beta \in [0.3, 0.7]$. RMSE has a large flat area, so that the alternative domain of two kernel parameters is still relatively large. The parameters α and β are robust under NLOS scenario. If the parameter α is greater than 5, RMSE will gradually increases. At the same time, with the increase of parameter α , the computational complexity will increase relatively. Therefore, according to the practical environment, the optimal parameter α should be no more than 5.

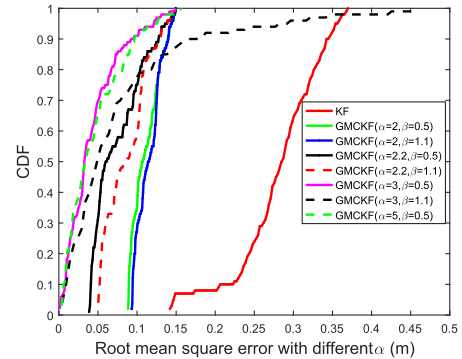


FIGURE 10. The effect of different parameters α under NLOS condition.

To further illustrate the impact of α , we select two fixed values β . Fig.10 shows that when $\beta = 0.5$ and α sets 3 or 5, GMCKF can produce smaller RMSE. Due to the effect of NLOS, the traditional KF has larger RMSE, and the algorithm does not achieve convergence. GMCKF is degraded to MCCKF with $\alpha = 2$. Although GMCKF can also converge, RMSE of $\alpha = 2$ is larger than that of $\alpha = 3$. Therefore, When the parameters α and β are suitably selected, GMCKF can reach a better performance than MCCKF.

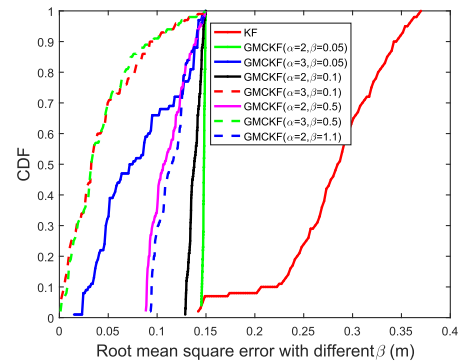


FIGURE 11. The effect of different parameters β under NLOS condition.

In addition, under the condition of fixed parameter $\alpha = 2$ and $\alpha = 3$, the effect of different parameters β is tested respectively. From Fig.9 and Fig.11, if the parameter β is too large, the abnormal NLOS errors cannot be effectively suppressed which leads to the poor performance.

2) STEADY-STATE PERFORMANCE UNDER LOS CONDITION
The effect of kernel parameters α and β is also verified under the LOS condition. From Fig.12, when the fixed parameter β

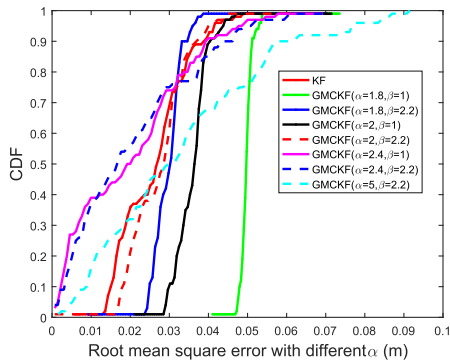


FIGURE 12. The effect of different parameters α under LOS condition.

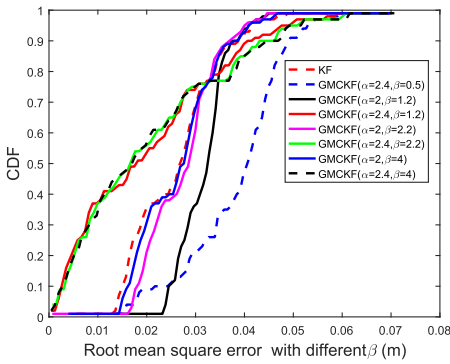


FIGURE 13. The effect of different parameters β under LOS condition.

is 1 or 2.2 and α is 2.4, 80% of RMSE of GMCKF keeps a small value. As shown in Fig.13, when the fixed parameter α is 2.4, GMCKF have the approximately same performance with $\beta \in \{1.2, 2.2, 4\}$ which is better than the traditional KF. However, if the parameters are not suitably selected, the performance of GMCKF will be worse. For example, GMCKF is degraded to MCCKF, and the performance with parameters $\alpha = 2$ and $\beta = 1.2$ is slightly worse than that of KF.

By testing kernel parameters α and β under NLOS and LOS condition, the optimal ranges of parameters are different, which are related to the practical environment. When kernel parameters are too large, GMCC is insensitive to some outliers and reduces the steady-state performance. When kernel parameters are too small, GMCC ignores the contribution of the useful information, and then results in performance degradation. From Fig.9-Fig.13, the performance of GMCKF is very close to that of KF under LOS condition, and better than that of KF under NLOS condition. In conclusion, GMCKF has a wider range of applications.

3) PERFORMANCE OF DIFFERENT ALGORITHMS UNDER NLOS CONDITION

We also test the performance of GMCKF with $\alpha = 3$ and $\beta = 0.5$ under NLOS condition. In order to ensure the consistency, GMCKF has the same parameter β as modified

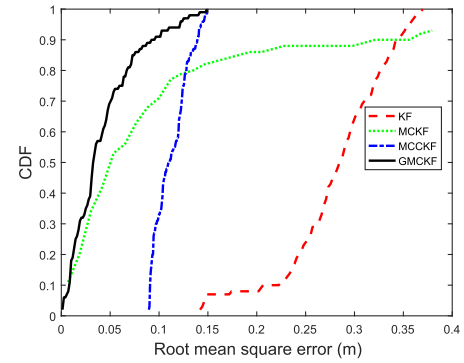


FIGURE 14. CDF of four algorithms under NLOS condition.

correntropy Kalman filter (MCKF) [14], MCCKF [14]. Fig.14 shows that GMCKF has smaller error than the other algorithms. When a large outlier occurs suddenly, the error of KF will become large. The errors of MCKF is relatively small in most cases, but some larger outliers still cannot be suppressed. The stability of MCKF is poor and is easily affected by NLOS. All errors of GMCKF are less than 0.1m due to the selection of appropriate kernel parameters. GMCKF is equal to MCCKF when $\alpha = 2$. For traditional KF and modified KF, the gain K_k indicates the predicted value x_k is closer to either state value or measurement value, thus ensuring that the predicted value is closer to the real value. For modified KF, the key of suppressing NLOS errors is whether the gain K_k can effectively reflect the error distribution characteristics. When the measurement value contains a large NLOS ranging, the predicted value approaches state value.

The gain K_k of MCCKF is associated with the residual error $y_k - Hx_{k|k-1}$ and β . However, the gain K_k of GMCKF is associated with the residual error $y_k - Hx_{k|k-1}$, β and α which has strong dynamic adjustment ability. When NLOS has different error distributions in the practical environment, the appropriate parameter α of GMCKF can be more effective to adjust the gain K_k , which makes the gain K_k be related to error distribution. Thus, the predicted value can be close to the real value, and the NLOS errors can be restrained eventually. Therefore, GMCKF has better performance than MCCKF with suitable parameter α .

4) PERFORMANCE OF DIFFERENT ALGORITHMS UNDER LOS CONDITION

In order to prove the generality, we test the performance of KF, MCKF, MCCKF and GMCKF under LOS condition. According to the result of experiment 2, kernel parameters are selected as $\alpha = 2.4$ and $\beta = 2$, respectively. From Fig.15, the performance of GMCKF is superior to the other three algorithms. 95% of RMSE of GMCKF is less than 0.05m. Because the effect of covariance matrix is not considered, MCKF cannot reach steady-state convergence. Meanwhile, when the parameter β is set to 2, MCCKF has a slightly worse performance as the traditional KF that can also result a small RMSE.

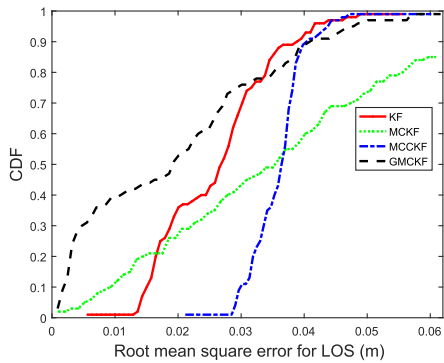


FIGURE 15. CDF of four algorithms under LOS condition.

5) COMPARISON OF RMSE AND COMPLEXITY OF ALGORITHMS

We also test RMSE and complexity under the three scenarios. It can be seen from Table 1 that the RMSE of GMCKF is smaller than that of the other three algorithms. Because GMCKF can effectively adjust two parameters, it has more robust against errors than MCCKF. In terms of cost of running time, although the overhead of the GMCKF is larger than that of MCKF, it has the similar complexity to KF.

TABLE 1. Comparison of RMSE and cost values under three typical scenarios (RMSE (m), cost ($\times 10^{-4}$ s)).

Scenario	Scenario 1		Scenario 2		Scenario 3	
	RMSE	Cost	RMSE	Cost	RMSE	Cost
KF	0.2808	0.38	0.0267	0.39	0.1706	0.39
MCKF	0.1281	0.15	0.0374	0.15	0.1073	0.15
MCCKF	0.1126	0.39	0.0364	0.39	0.0911	0.39
GMCKF	0.0430	0.41	0.0200	0.41	0.0393	0.41

C. PRACTICAL LOCALIZATION PERFORMANCE

In this section, we apply ranging results of GMCKF to different localization algorithms, that is, trilateration localization, maximum likelihood localization (ML), and total least squares (TLS). And, the validity of GMCKF algorithm is verified by the practical scenario.

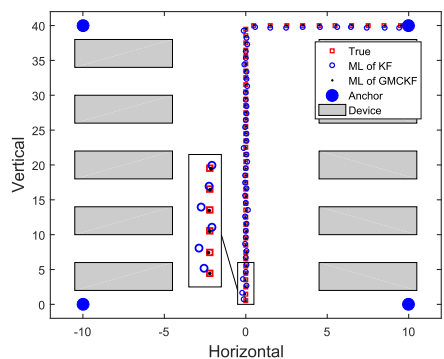


FIGURE 16. Localization accuracy of ML with KF and GMCKF algorithms.

As is shown in Fig.16, the factory field is $44m \times 24m$. The four anchor nodes are located in the corner of region which

are $(-10m, 0m)$, $(10m, 0m)$, $(-10m, 40m)$, $(10m, 40m)$ and represented as four blue disks. The gray boxes are the devices. The whole scenario is equivalent to above scenario 3 above which has NLOS and LOS conditions. The tag node which moves with uniform speed communicates with four anchor nodes at each moment.

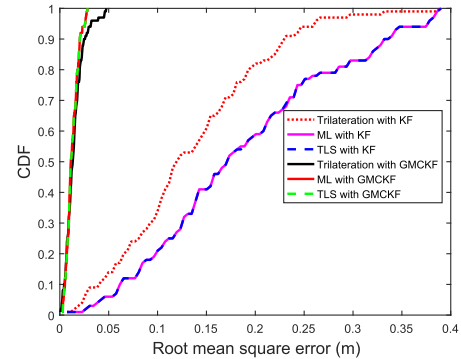


FIGURE 17. RMSE of localization for three algorithms.

TABLE 2. RMSE of Localization performance with KF and GMCKF (m).

	KF	GMCKF
Trilateration	0.1548	0.0175
ML	0.1376	0.0143
TLS	0.1376	0.0143

Fig.16 indicates GMCKF algorithm can effectively eliminate the errors of the NLOS condition and make localization results closer to the actual location. ML localization with GMCKF has better performance than that with KF at some times. Fig.17 also shows that RMSE of three different localization algorithms with GMCKF has smaller errors. ML and TLS show the same performance with GMCKF. The localization errors of three different algorithms with GMCKF is less than 0.05m. However, some localization errors of the three different algorithms with KF are greater than 0.3m which cannot be ignored. Table 2 also shows that GMCKF is more robust than KF with three common localization algorithms. GMCKF can effectively deal with all kinds of scenarios.

VI. CONCLUSION

Aiming at the problem that the ranging accuracy of UWB is significantly affected by NLOS errors, we propose the generalized maximum correntropy Kalman filter (GMCKF) algorithm by using GMCC as the cost function. When the ranging results contain large outliers, GMCC can effectively suppress the gain matrix in Kalman filter, and then ensure smoothing filtering. GMCKF is applied to the typical industrial factory, and the steady-state performance of GMCKF is proved. Finally, we verify that this proposed algorithm is superior to KF, MCKF and MCCKF in the industrial environment.

ACKNOWLEDGMENT

(Fuqiang Ma and Jie He are co-first authors.)

REFERENCES

- [1] C. Xu, J. He, X. Zhang, P.-H. Tseng, and S. Duan, "Toward near-ground localization: Modeling and applications for TOA ranging error," *IEEE Trans. Antennas Propag.*, vol. 65, no. 10, pp. 5658–5662, Oct. 2017.
- [2] C. Xu, J. He, X. Zhang, C. Yao, and P.-H. Tseng, "Geometrical kinematic modeling on human motion using method of multi-sensor fusion," *Inf. Fusion*, vol. 41, pp. 243–254, May 2018.
- [3] F. Ma, F. Liu, X. Zhang, P. Wang, H. Bai, and H. Guo, "An ultrasonic positioning algorithm based on maximum correntropy criterion extended Kalman filter weighted centroid," *Signal, Image Video Process.*, vol. 12, no. 6, pp. 1207–1215, 2018.
- [4] X. Wu, R. Shen, L. Fu, X. Tian, P. Liu, and X. Wang, "iBILL: Using iBeacon and inertial sensors for accurate indoor localization in large open areas," *IEEE Access*, vol. 5, pp. 14589–14599, 2017.
- [5] D. Cassioli, M. Z. Win, and A. F. Molisch, "The ultra-wide bandwidth indoor channel: From statistical model to simulations," *IEEE J. Sel. Areas Commun.*, vol. 20, no. 6, pp. 1247–1257, Aug. 2002.
- [6] S. S. Ghassemzadeh, R. Jana, C. W. Rice, W. Turin, and V. Tarokh, "Measurement and modeling of an ultra-wide bandwidth indoor channel," *IEEE Trans. Commun.*, vol. 52, no. 10, pp. 1786–1796, Oct. 2004.
- [7] C.-C. Chong, Y.-E. Kim, S. K. Yong, and S.-S. Lee, "Statistical characterization of the UWB propagation channel in indoor residential environment," *Wireless Commun. Mobile Comput.*, vol. 5, no. 5, pp. 503–512, 2005.
- [8] R.-R. Lao, J.-H. Targ, and C. Hsiao, "Transmission coefficients measurement of building materials for UWB systems in 3–10 GHz," in *Proc. Veh. Technol. Conf.*, vol. 1, Apr. 2003, pp. 22–25.
- [9] S. Marano, W. M. Gifford, H. Wymeersch, and M. Z. Win, "NLOS identification and mitigation for localization based on UWB experimental data," *IEEE J. Sel. Areas Commun.*, vol. 28, no. 7, pp. 1026–1035, Sep. 2010.
- [10] J. He, Y. Geng, F. Liu, and C. Xu, "CC-KF: Enhanced TOA performance in multipath and NLOS indoor extreme environment," *IEEE Sensors J.*, vol. 14, no. 11, pp. 3766–3774, Nov. 2014.
- [11] Z. Xiong, F. Sottile, R. Garello, and C. Pastone, "A cooperative NLoS identification and positioning approach in wireless networks," in *Proc. IEEE Int. Conf. Ultra-Wideband (ICUWB)*, Sep. 2014, pp. 19–24.
- [12] D.-C. Chang, "Time-of-arrival motion positioning with the new concatenated IMM method," in *Proc. IEEE Globecom Workshops (GC Wkshps)*, Dec. 2015, pp. 1–6.
- [13] J. Zhao and H. Zhang, "Kernel recursive generalized maximum correntropy," *IEEE Signal Process. Lett.*, vol. 24, no. 12, pp. 1832–1836, Dec. 2017.
- [14] R. Izanloo, S. A. Fakoorian, H. S. Yazdi, and D. Simon, "Kalman filtering based on the maximum correntropy criterion in the presence of non-Gaussian noise," in *Proc. Annu. Conf. IEEE Inf. Sci. Syst. (CISS)*, Mar. 2016, pp. 500–505.
- [15] B. Chen, L. Xing, H. Zhao, N. Zheng, and J. C. Príncipe, "Generalized correntropy for robust adaptive filtering," *IEEE Trans. Signal Process.*, vol. 64, no. 13, pp. 3376–3387, Jul. 2016.
- [16] J. A. Santana, E. Macías, Á. Suárez, D. Marrero, and V. Mena, "Adaptive estimation of WiFi RSSI and its impact over advanced wireless services," *Mobile Netw. Appl.*, vol. 22, no. 6, pp. 1100–1112, 2017.
- [17] M. R. Gholami, S. Gezici, and E. G. Ström, "TW-TOA based positioning in the presence of clock imperfections," *Digit. Signal Process.*, vol. 59, pp. 19–30, Dec. 2016.
- [18] X. Qu, L. Xie, and W. Tan, "Iterative constrained weighted least squares source localization using TDOA and FDOA measurements," *IEEE Trans. Signal Process.*, vol. 65, no. 15, pp. 3990–4003, May 2017.
- [19] Y. S. Lee, J. W. Park, and L. Barolli, "A localization algorithm based on AOA for ad-hoc sensor networks," *Mobile Inf. Syst.*, vol. 8, no. 1, pp. 61–72, 2012.
- [20] J. M. Huerta, J. Vidal, A. Giremus, and J.-Y. Tourneret, "Joint particle filter and UKF position tracking in severe non-line-of-sight situations," *IEEE J. Sel. Topics Signal Process.*, vol. 3, no. 5, pp. 874–888, Oct. 2009.
- [21] I. Guvenc, C. C. Chong, and F. Watanabe, "NLOS identification and mitigation for UWB localization systems," in *Proc. IEEE Wireless Commun. Netw. Conf. (WCNC)*, Mar. 2007, pp. 1571–1576.
- [22] S. F. A. Shah and A. H. Tewfik, "Performance analysis of directional beacon based position location algorithm for UWB systems," in *Proc. IEEE Global Telecommun. Conf. (GLOBECOM)*, Dec. 2005, pp. 1–5.
- [23] A. De Angelis, S. Dwivedi, and P. Hänel, "Characterization of a flexible UWB sensor for indoor localization," *IEEE Trans. Instrum. Meas.*, vol. 62, no. 5, pp. 905–913, May 2013.
- [24] J. Yan, C. J. M. Tiberius, G. Bellusci, and G. J. M. Janssen, "Non-line-of-sight identification for indoor positioning using ultra-WideBand radio signals," *Navigation*, vol. 60, no. 2, pp. 97–111, 2013.
- [25] K. Yu and E. Dutkiewicz, "NLOS identification and mitigation for mobile tracking," *IEEE Trans. Aerosp. Electron. Syst.*, vol. 49, no. 3, pp. 1438–1452, Jul. 2013.
- [26] X. Jiang and H. Zhang, "Non-line of sight error mitigation in UWB ranging systems using information fusion," in *Electronics and Signal Processing*. Berlin, Germany: Springer, 2011, pp. 969–976.
- [27] S. Bartoletti, A. Giorgetti, M. Z. Win, and A. Conti, "Blind selection of representative observations for sensor radar networks," *IEEE Trans. Veh. Technol.*, vol. 64, no. 4, pp. 1388–1400, Apr. 2015.
- [28] S. Bartoletti, W. Dai, A. Conti, and M. Z. Win, "A mathematical model for wideband ranging," *IEEE J. Sel. Topics Signal Process.*, vol. 9, no. 2, pp. 216–228, Mar. 2015.
- [29] F. Montorsi, F. Pancaldi, and G. M. Vitetta, "Statistical characterization and mitigation of NLOS errors in UWB localization systems," in *Proc. IEEE Int. Conf. Ultra-Wideband (ICUWB)*, Sep. 2011, pp. 86–90.
- [30] H. Wymeersch, S. Marano, W. M. Gifford, and M. Z. Win, "A machine learning approach to ranging error mitigation for UWB localization," *IEEE Trans. Commun.*, vol. 60, no. 6, pp. 1719–1728, Jun. 2012.
- [31] W. Li, Y. Jia, and J. Du, "TOA-based cooperative localization for mobile stations with NLOS mitigation," *J. Franklin Inst.*, vol. 353, no. 6, pp. 1297–1312, Apr. 2016.
- [32] U. Hammes and A. M. Zoubir, "Robust MT tracking based on M-estimation and interacting multiple model algorithm," *IEEE Trans. Signal Process.*, vol. 59, no. 7, pp. 3398–3409, Jul. 2011.
- [33] G. Wang, N. Li, and Y. Zhang, "Maximum correntropy unscented Kalman and information filters for non-Gaussian measurement noise," *J. Franklin Inst.*, vol. 354, no. 18, pp. 8659–8677, 2017.
- [34] L. N. Guo, Y. Ding, Z. Wang, G. S. Xu, and B. Wu, "A dynamic load estimation method for nonlinear structures with unscented Kalman filter," *Mech. Syst. Signal Process.*, vol. 101, pp. 254–273, Feb. 2018.
- [35] P. Yang, "Efficient particle filter algorithm for ultrasonic sensor-based 2D range-only simultaneous localisation and mapping application," *IET Wireless Sensor Syst.*, vol. 2, no. 4, pp. 394–401, Dec. 2012.
- [36] P. Ciosas and J. Vila-Valls, "NLOS mitigation in TOA-based indoor localization by nonlinear filtering under skew t-distributed measurement noise," in *Proc. IEEE Stat. Signal Process. Workshop (SSP)*, Jun. 2016, pp. 1–5.
- [37] B. Chen, X. Liu, H. Zhao, and J. C. Príncipe, "Maximum correntropy Kalman filter," *Automatica*, vol. 76, pp. 70–77, Feb. 2017.
- [38] G. M. Khan, A. A. Ashraf, J. Käredal, F. Tufvesson, and A. Molisch, "Measurements and analysis of UWB channels in industrial environments," in *Proc. Int. Symp. Wireless Pers. Multimedia Commun. (WPMC)*, 2005, pp. 426–430.
- [39] M. A. Landolsi, A. H. Muqaibel, and A. F. Almutairi, "UKF-based channel estimation and LOS/NLOS classification in UWB wireless networks," *J. Eng. Res.*, vol. 4, no. 2, pp. 1–17, 2016.
- [40] M. Ridolfi, S. Van de Velde, H. Steendam, and E. De Poorter, "Analysis of the scalability of UWB indoor localization solutions for high user densities," *Sensors*, vol. 18, no. 6, p. 1875, 2018.
- [41] H. Ko, B. Kim, and S.-H. Kong, "GNSS multipath-resistant cooperative navigation in urban vehicular networks," *IEEE Trans. Veh. Technol.*, vol. 64, no. 12, pp. 5450–5463, Dec. 2015.
- [42] Y. Zhao, Y. Yang, and M. Kyas, "Adaptive range-based nonlinear filters for wireless indoor positioning system using dynamic Gaussian model," *IEEE Trans. Veh. Technol.*, vol. 64, no. 9, pp. 4282–4291, Sep. 2015.
- [43] F. A. Ghaled, A. Zainal, M. A. Rassam, and A. Abraham, "Improved vehicle positioning algorithm using enhanced innovation-based adaptive Kalman filter," *Pervas. Mobile Comput.*, vol. 40, pp. 139–155, Sep. 2017.



FUQIANG MA received the B.E. degree in computer science and technology from the University of Science and Technology Beijing, China, in 2015, where he is currently pursuing the Ph.D. degree. His research interests include wireless sensor networks, pattern recognition, array signal processing, and machine learning.



JIE HE received the B.E. and Ph.D. degrees from the University of Science and Technology Beijing, Beijing, China, in 2005 and 2012, respectively, where he is currently an Associate Professor with the School of Computer and Communication Engineering and a Researcher of the Data and Cyber-Physical System Laboratory. His current research interests include indoor location systems, wireless sensor networks, and body area networks.



XIAOTONG ZHANG received the M.E. and Ph.D. degrees from the University of Science and Technology Beijing, in 1997 and 2000, respectively. He was a Professor with the Department of Computer Science and Technology, University of Science and Technology Beijing. His industry experience includes affiliation with Beijing BM Electronics High-Technology Co., Ltd. from 2002 to 2003, where he involved in digital video broadcasting communication systems and IC design. His industrial cooperation experience includes BLX IC Design Co., Ltd, North Communications Corporation of PetroChina, and Huawei Technologies Co., Ltd. His research interests include quality of wireless channels and networks, wireless sensor networks, networks management, cross-layer design and resource allocation of broadband and wireless networks, signal processing of communication, and computer architecture.

• • •